A stochastic spatiotemporal model of a response-regulator network in the *Caulobacter crescentus* cell cycle

IOP Publishing Phys. Biol. 13 (2016) 035007 doi:10.1088/1478-3975/13/3/035007

Physical Biology

PAPER

RECEIVED
8 December 2015

REVISED
9 May 2016

ACCEPTED FOR PUBLICATION
19 May 2016

PUBLISHED
24 June 2016

A stochastic spatiotemporal model of a response-regulator network in the *Caulobacter crescentus* cell cycle

Fei Li[1], **Kartik Subramanian**[2], **Minghan Chen**[1], **John J Tyson**[2] **and Yang Cao**[1]

[1] Departments of Computer Science, Virginia Tech, Blacksburg, VA 24061,USA
[2] Biological Sciences Virginia Tech, Blacksburg, VA 24061,USA

E-mail: felix@vt.edu, skartik@vt.edu, tyson@vt.edu and ycao@vt.edu

Keywords: *Caulobacter crescentus*, cell cycle, stochastic model and simulation, reaction diffusion system

Abstract

The asymmetric cell division cycle in *Caulobacter crescentus* is controlled by an elaborate molecular mechanism governing the production, activation and spatial localization of a host of interacting proteins. In previous work, we proposed a deterministic mathematical model for the spatiotemporal dynamics of six major regulatory proteins. In this paper, we study a stochastic version of the model, which takes into account molecular fluctuations of these regulatory proteins in space and time during early stages of the cell cycle of wild-type *Caulobacter* cells. We test the stochastic model with regard to experimental observations of increased variability of cycle time in cells depleted of the *divJ* gene product. The deterministic model predicts that overexpression of the *divK* gene blocks cell cycle progression in the stalked stage; however, stochastic simulations suggest that a small fraction of the mutants cells do complete the cell cycle normally.

1. Introduction

Caulobacter crescentus is an aquatic α-proteobacterium that is widely distributed in freshwater lakes and streams [26]. As illustrated in figure 1, *Caulobacter* cells divide asymmetrically [6, 10, 38, 40]. The larger cell, called the stalked cell, is anchored to its substratum by a stalk and holdfast. The stalked cell is able to initiate chromosome replication and begin the division-differentiation cycle immediately. The smaller cell, called the swarmer cell, is equipped with a polar flagellum and several pili, with which it swims away from its place of birth. The swarmer cell is not competent for chromosome replication and cell division until it differentiates into a stalked cell. The swarmer-to-stalked transition involves shedding the flagellum, retracting the pili, and constructing a stalk in their place. The stalked cell grows primarily in length (slightly banana-shaped) and eventually builds a flagellum at the 'new' pole (the pole derived from the septum at the previous division). After chromosome replication and segregation is completed, a ring of tubulin-like proteins (FtsZ) constricts and divides the cytoplasm into two separate compartments [24]. Cytoplasmic compartmentalization enables divergent programs of cell differentiation, yielding two distinct progeny: a stalked cell and a swarmer cell.

Asymmetric cell division is a common feature of cell proliferation in many types of organisms [11, 32, 36, 37, 42, 49]. Typical of these situations, the asymmetric division-differentiation cycle of *Caulobacter crescentus* involves an elaborate sequence of spatiotemporally regulated protein interactions that control chromosome segregation, polar differentiation and regulator localization [3, 25]. Experimentalists have identified four 'master regulators' of the *Caulobacter* cell cycle, namely DnaA, GcrA, CtrA and CcrM, which determine the temporal expression of approximately 200 genes [8, 9, 16]. These master transcription regulators oscillate temporally and spatially and drive a series of modular functions during the cell cycle. The molecular mechanisms governing CtrA functions have been studied in great detail, but the controls of DnaA, GcrA and CcrM are less well known.

In swarmer cells, CtrA is phosphorylated by a phosphorelay system (CckA and ChpT) [5, 7]. Phosphorylated CtrA (CtrAp) binds to the chromosomal origin of replication (*Cori*) and inhibits the initiation of chromosome replication [39]. During the swarmer-to-stalked transition, CtrAp gets dephosphorylated and degraded, allowing the initiation of chromosome

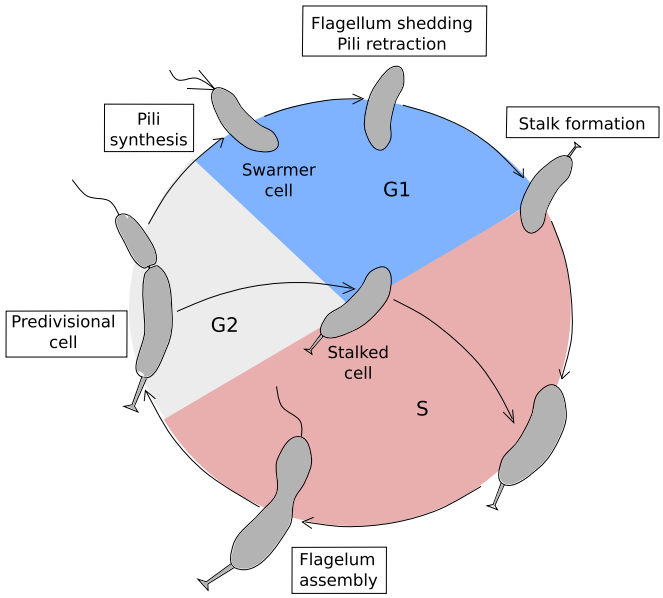

Figure 1. The asymmetric division cycle of *Caulobacter* cells, redrawn from an original figure by Christine Jacobs-Wagner.

replication. CtrA is degraded by an ATP-dependent protease, ClpXP [22, 30], which is localized to the stalk pole by the unphosphorylated response regulator CpdR. As the nascent stalked cell progresses through the replication-division cycle, CpdR is phosphorylated by CckA-ChpT, loses it polar localization, and, consequently, loses its ability to recruit ClpXP protease for CtrA degradation. In addition, CckA-ChpT phosphorylate and reactivate CtrA [18]. Although the mechanisms connecting CckA to CtrA functions have been identified, the pathways for CckA localization and regulation are still unclear.

Development of the flagellated pole is controlled by the phosphorylation state of DivK in response to the histidine kinase DivJ and the bifunctional histidine kinase/phosphatase PleC [17]. The DivJ–PleC–DivK pathway regulates the phosphorylation status of PleD, which governs polar development, such as flagellum shedding and stalk biosynthesis [34]. At the swarmer-to-stalked transition, PleD is phosphorylated by PleC kinase and localized at the stalk pole. Localized PleD induces the synthesis of the second messenger, cyclic di-GMP, to signal stalk development [1, 12, 33]. The non-canonical histidine kinase, DivL [47], promotes CckA kinase activity. CckA kinase phosphorylates and activates CtrA in the swarmer cell. In the stalked cell, phosphorylated DivK binds to DivL and inhibits CckA kinase activity. During the swarmer- to-stalked transition, DivJ phosphorylates DivK. Phosphorylated DivK in turn binds and inhibits DivL, thereby inhibiting CckA kinase activity. Subsequent dephosphorylation and degradation of CtrA allows the initiation of chromosome replication.

As the cell progresses into the previsional stage, PleC accumulates at the new pole. While the bifunctionality of CckA as a phosphatase and kinase is well known, the potential bifunctionality of PleC as a histidine phosphatase/kinase in predivisional cells has been under debate for some time [44]. Experiments [2, 33] show that phosphorylated DivK (DivKp) upregulates the kinase form of PleC. By phosphorylating PleD, PleC kinase initiates the pathway for stalk pole development. This view of PleC as a kinase at the old pole raises a question of what is happening at the new pole of predivisional cells (the nascent swarmer pole). The canonical view [29, 47] suggests that in the predivisional cell PleC functions as a phosphatase at the new pole, where it dephosphorylates DivK and creates a protection zone for active DivL, active CckA, and CtrA phosphorylation. An alternate view is that PleC remains a kinase in previsional cells. However, this raises the question of how DivL is protected form the inhibitory effect of DivKp. Recently, using a mathematical model (reaction–diffusion equations) of the DivJ–PleC–DivK and DivL–CckA–CtrA network, Subramanian *et al* [44] provided support for the view that PleC is a kinase at the new pole. Their simulations show that PleC kinase at the new pole of a predivisional cell can sequester DivKp from binding to DivL. Free DivL upregulates CckA, thereby promoting phosphorylation of CtrA and the formation of CtrAp gradient in the predivisional cell. After constriction of the FtsZ ring, compartmentalization of the predivisional cell separates PleC kinase at the new pole from DivJ kinase at the old pole. PleC reverts back to a phosphatase. As a consequence, DivK is dephosphorylated in the swarmer cell compartment, while phosphorylated DivK is retained in the stalked cell compartment.

Although cell cycle progression in *Caulobacter* is robust in respect to protein regulation and the proper sequence of events, cells exhibit considerable variability in other respects, such as the times spent in

various phases of the cycle and the sizes of cells at the time events occur [28]. These variabilities in cell cycle progression are attributable in large part to the fact that the populations of protein species in a single *Caulobacter* cell are limited in number and therefore subject to random molecular fluctuations. For example, the volume of a *Caulobacter* cell is roughly 1 fL at division and contains ∼300 molecules of a particular protein species (if its concentration is ∼500 nmol l^{-1}). Moreover, the number of mRNA molecules for each protein at any time is likely to be ∼10 [45]. With such numbers of mRNAs and proteins, molecular fluctuations at the protein level are expected to be ∼25% [35]. Such large fluctuations in protein levels may significantly affect the properties of the cell cycle control system. For example, recent optical microscopy measurements reveal an intriguing role of DivJ in the control of noise in single *Caulobacter* cells [41]: the data show that depleting cells of DivJ causes (in addition to a modest increase of ∼16 min in mean interdivision time) a large increase in the variance of interdivision times (the coefficient of variation of interdivision times increases from ∼11% for wild-type cells to ∼26% for *divJ*-deleted cells).

The authors of this study, Lin *et al* [28], proposed a simplified protein interaction network that captures the noisy oscillations of protein abundances during the *Caulobacter* cell cycle and accounts for their observations of the variability of cell cycle periods in wild-type and *divJ*-deleted cells. Lin *et al*'s model is illuminating, but it suffers some shortcomings: it does not take into account the effects of fluctuations at the mRNA level or of the spatial distributions of the regulatory proteins, and it relies on a 'non-detailed' simulation of stochastic processes. In this paper, we avoid these shortcomings by extending the deterministic reaction–diffusion model of Subramanian *et al* [44] to a mechanistically detailed, spatiotemporal, stochastic model, including mRNA species. With this model we investigate the effects of *divJ* deletion and *divK* overexpression on cell cycle progression in single *Caulobacter* cells. Our simulations of the *divJ*-deletion strain are consistent with the observations of Lin *et al* [28], and our simulations of *divK*-overexpression strains predict a stochastic phenotype of these cells: although most cells are blocked in the stalked stage of the cell cycle (as predicted by the deterministic model of Subramanian *et al* [44]), some cells are able to complete the cell cycle normally.

2. Method

2.1. Stochastic model

In previous work [44], we proposed a deterministic mathematical model for the spatiotemporal dynamics of six regulatory proteins during the *Caulobacter* cell cycle. Figure 2 shows the regulatory network of these proteins. PleC acts as a bifunctional histidine kinase/phosphatase, catalyzing the transformations between DivK and DivKp [43]. Significantly, DivKp up-regulates the kinase activity of PleC [33]. Figure A1 (in the appendix) shows the detailed scheme of PleC transformations between phosphatase and kinase, depending on how the various forms of PleC are bound to DivK and DivKp. Our spatial stochastic model is based on this reaction network.

The activation of CckA kinase by DivL is described in our model by a Hill function (this is the only aspect of the model that is not described by mass-action kinetics). CtrA is phosphorylated by CckA kinase, and dephosphorylated by CckA phosphatase. Linkage between the DivJ–DivK–PleC and Div–CckA–CtrA modules is achieved by the binding of DivKp to DivL, which prevents DivL from upregulating the kinase activity of CckA. The state of CtrA serves as the final output signal of our model.

The deterministic spatiotemporal model [44] robustly captures the localization and activities of the regulatory proteins. However, it cannot capture the molecular noise intrinsic to the reaction network. In this paper we build a discrete stochastic model based on the deterministic model and study noise in protein populations and cell cycle periods. In addition to the protein dynamics of the original model, we also take into account the dynamics of genes (*divJ, divK, divL, pleC, cckA, ctrA*) and mRNAs, to determine how fluctuations at the level of nucleic acids affects fluctuating protein levels during the *Caulobacter* cell cycle. Table A1 (appendix) provides a complete list of reactions and propensities for our model.

As explained in 'model details' (appendix), we enforce several discrete events on the reaction–diffusion equations governing DivJ, DivK, DivL, PleC, CckA and CtrA. In paticular, we use'localization indicator functions' (see figure A2 in appendix) to force DivJ, PleC, DivL and CckA molecules to become localized to specific places in the cell in specific stages of the cell cycle, based on experimental observations on wild-type cells.

2.2. Stochastic simulation algorithm (SSA)

Gillespie's SSA [14, 15] is one of the most widely used stochastic simulation methods for 'well-stirred' biochemical systems. In each step, SSA answers two questions: when (τ) will the next reaction fire and which reaction (index j) will fire. For a well-stirred system, the direct SSA method yields

$$\tau = \frac{1}{a_0(x)} \ln\left(\frac{1}{r_1}\right)$$
$$j = \text{the smallest integer satisfying } \sum_{j'=1}^{j} a_{j'}(x) > r_2 a_0(x), \quad (1)$$

where r_1 and r_2 are two uniform random variables in (0, 1), $a_j(x)$ is the reaction propensity of the jth

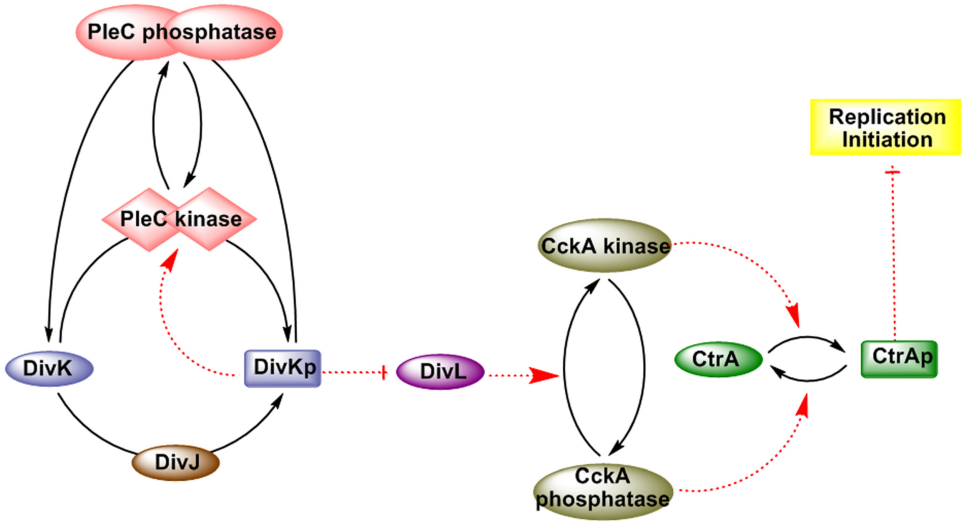

Figure 2. Regulatory network of two phosphorelay systems that play major roles in the cell division cycle of *Caulobacter crescentus*. The phosphorylated form of CtrA inhibits the initiation of chromosome replication in swarmer cells. The phosphorylated form of DivK indirectly inhibits the phosphorylation of CtrA, through the DivL–CckA pathway. The kinase activity of the enzyme, PleC, is up-regulated by the product, DivKp, of the kinase reaction.

Table 1. The mean and variance of the swarmer-to-stalked transition times in wild-type and *divJ* deletion cells.

SW-to-ST time	Wild type	$\Delta divJ$
Mean	42 min	49 min
Variance	35 min^2	225 min^2
COV	14%	29%

reaction and $a_0(x) = \sum_{j=1}^{M} a_j(x)$ is the total reaction propensity of all M reaction channels.

For reaction–diffusion (RD) systems, the 'well-stirred' assumption is not valid and Gillespie's direct SSA method cannot be applied. A common practice is to discretize the spatial domain according to the reaction diffusion master equation (RDME) framework [13, 19]. The key assumption of the RDME is that all species in each compartment are well-stirred. In this case, chemical reactions in each compartment can be simulated by the SSA and diffusion can be modeled as random walk among neighboring compartments. If the discretization size is h, the propensity for one molecule to jump to one of its nearest neighbors is given by D/h^2, where D is the diffusion rate constant.

For *Caulobacter*, we model this banana shaped cell with a 1D domain along its long axis and discretize the corresponding 1D reaction–diffusion system into 50 compartments ('bins'), as in the RDME framework. In each compartment, all chemical reactions (listed in table A1) as well as all diffusive jumps (listed in table A2) are simulated by 'direct method' of SSA. During cell growth, we keep the number of bins constant but let the length of each bin increase exponentially with time. Please refer to the appendix for more details about the stochastic model and the stochastic simulation method.

3. Results

3.1. PleC kinase sequesters DivKp in the early predivisional stage

In the predivisional stage, active DivL at the new pole upregulates CckA kinase there, which promotes CtrA phosphorylation at the new pole. At the old pole, DivL is lacking and CckA is in the phosphatase form, dephosphorylating CtrA at the stalked end of the cell. These effects create a gradient of CtrA phosphorylation from the new pole toward the old pole of the early predivisional cell. This gradient is crucial for further asymmetric cell development. Early in the predivisional stage, PleC becomes localized to the new pole [46].

It is unclear if PleC in the predivisional stage is a phosphatase or a kinase [23, 46] Our deterministic model [44] showed that once PleC becomes a kinase in the stalked cell, it remains a kinase even in the predivisional cell. It is only after cytokinesis separates DivJ and PleC into separate compartments that PleC reverts back to a phosphatase. This result is counter-intuitive, because PleC kinase would be expected to phosphorylate DivK and DivKp would bind to and inhibit DivL (see figure 2). However, our simulations also showed that the DivKp is present in complex with PleC [43, 44]. Therefore, we hypothesized that the kinase form of PleC may sequester DivKp away from DivL.

Our stochastic simulations support this view. Figure 3 shows histograms of DivKp and DivL components in the early predivisional stage ($t = 120$ min). Most DivKp molecules are complexed with PleC, leaving DivL free to activate CckA kinase. Furthermore, our simulations are consistent with expectations of how protein populations will fluctuate during the

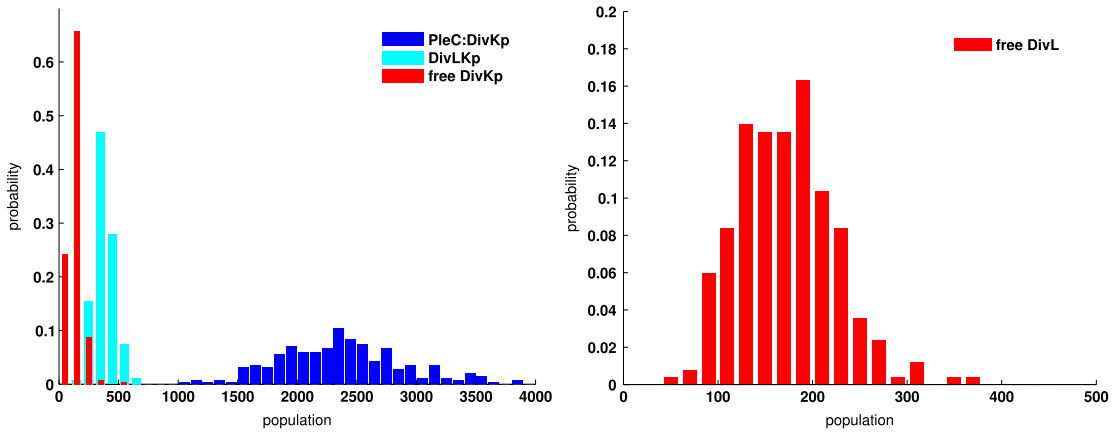

Figure 3. Histograms of DivKp and free DivL in the early predivisional stage of the *Caulobacter* cell cycle. Left: most DivKp molecules are complexed with PleC histidine kinase. Right: most DivL molecules are free to activate CckA kinase.

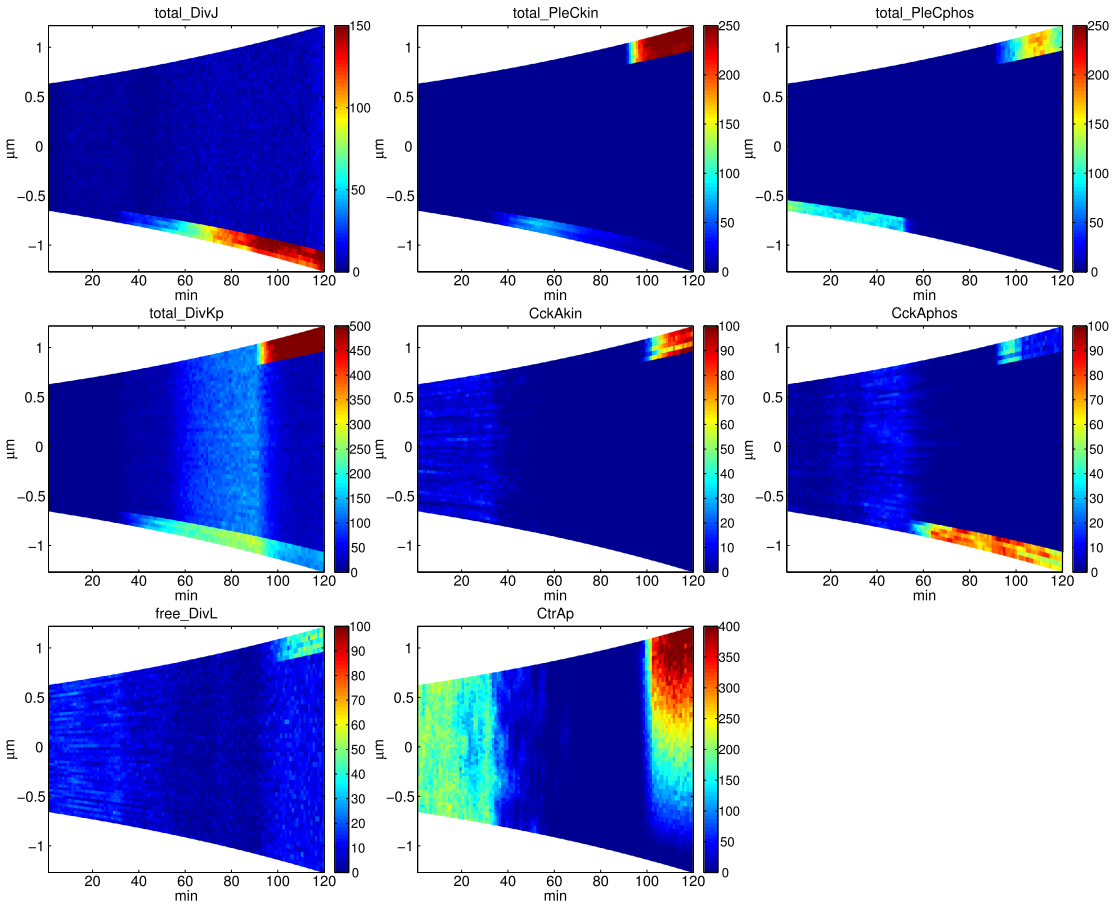

Figure 4. A typical stochastic simulation of regulatory proteins during the *Caulobacter* cell cycle prior to cytokinesis. Colors indicate the numbers of protein molecules in each bin. DivJ is synthesized throughout the cell cycle and becomes localized at the old pole after $t = 30$ min. Transient co-localization of DivJ and PleC ($t = 30$–50 min) turns PleC into kinase form, before PleC is cleared from the old pole ($t = 50$–90 min) and relocates ($t = 90$–120 min) to the new pole (the nascent flagellated pole). Upon phosphorylation, DivK localizes to the poles of the cell, where it binds with PleC histidine kinase. Despite the presence of phosphorylated DivK at the new pole of the predivisional cell, DivL stays active (free DivL, unbound to DivKp) because PleC kinase sequesters DivKp and prevents it from binding to DivL. In the swarmer stage, CckA is uniformly distributed and stays as the kinase form. In the predivisional stage, CckA localizes to both poles. Reactivation of DivL turns CckA into the kinase form at the swarmer pole, while CckA remains as a phosphatase at the stalk pole. Consequently, the late predivisional cell establishes a gradient of phosphorylated CtrA along its length with a high level of CtrAp at the new pole and a low level at the old pole. Our stochastic simulations generate temporally varying protein distributions similar to the results of the deterministic model [44] with realistic fluctuations superimposed.

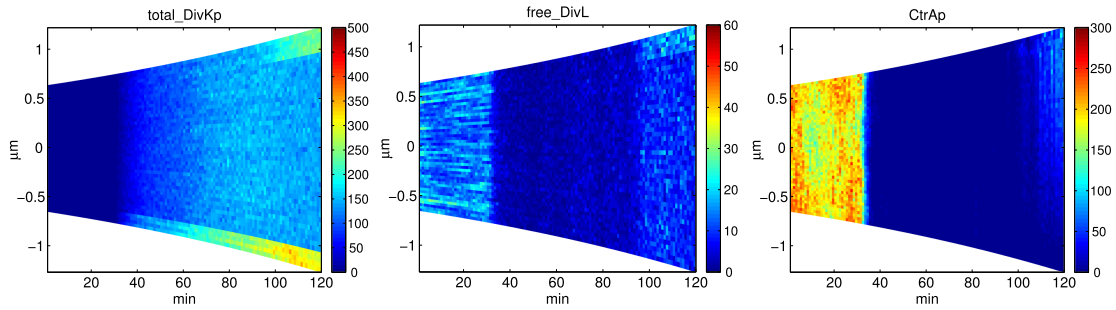

Figure 5. A typical stochastic simulation of certain regulatory proteins in the late pre-divisional stage of the *Caulobacter* cell cycle in the PleC deletion mutant case. Colors indicate the numbers of protein molecules in each bin.

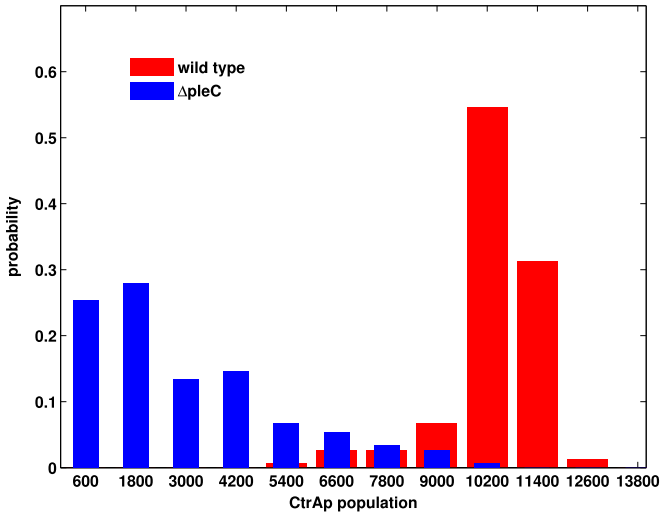

Figure 6. Histogram of CtrAp level at the predivisional stage for the PleC deletion mutant case.

division cycle of a wild-type cell, see figure 4. In our model, it takes 150 min for a newborn swarmer cell to proceed through the entire cycle and divide into a stalked cell and swarmer cell pair. In the swarmer stage of the cell cycle ($t = 0$–30 min), PleC is localized at the old pole and functions as a phosphatase. DivK is unphosphorylated and DivL is active; hence, CtrA is phosphorylated, and CtrAp inhibits the initiation of chromosome replication. During the swarmer-to-stalked transition ($t = 30$–50 min), DivJ becomes localized at the old pole and DivK is phosphorylated. DivKp inhibits DivL; hence, CckA becomes a phosphatase, CtrA is unphosphorylated, and the cell enters the stalked cell stage. Chromosome replication begins and the newly replicated chromosome is translocated to the new pole at $t = 50$ min (see 'model details' in appendix). PleC is cleared from the old pole in the stalked stage ($t = 50$–90 min) and relocates to the new pole in the early predivisional stage ($t = 90$–120 min).

pleC::Tn5 mutants are stalkless, have elevated level of DivKp, and significantly lower level of CtrAp. Interestingly, bipolar localization of DivKp is retained [21, 48]. Our simulations show that in the absence of PleC, DivKp can now bind to and inactivate DivL, causing loss of CtrAp (figure 5). In the predivisional stage, our simulations show that the CtrAp gradient is abolished, except in a small fraction of simulated cells where, due to random fluctuations, CtrAp level increases (figure 6).

Our stochastic simulations generate temporally varying protein distributions similar to the predictions of the deterministic model [44] with realistic fluctuations superimposed. Counter to intuitive expectations, it is not necessary for PleC to be a phosphatase at the new pole in order to establish high levels of phosphorylated CtrA in the swarmer half of the predivisional cell. Instead, PleC in the kinase form can sequester DivKp away from DivL, allowing free DivL to activate CckA kinase, which (indirectly) phosphorylates CtrA at the new pole.

3.2. Compartmentalization separates the functionality of DivJ and PleC

In our model, we enforce compartmentalization of the cell at $t = 120$ min by preventing the diffusion of proteins across the mid-cell line. Compartmentalization marks the transition from the early predivisional

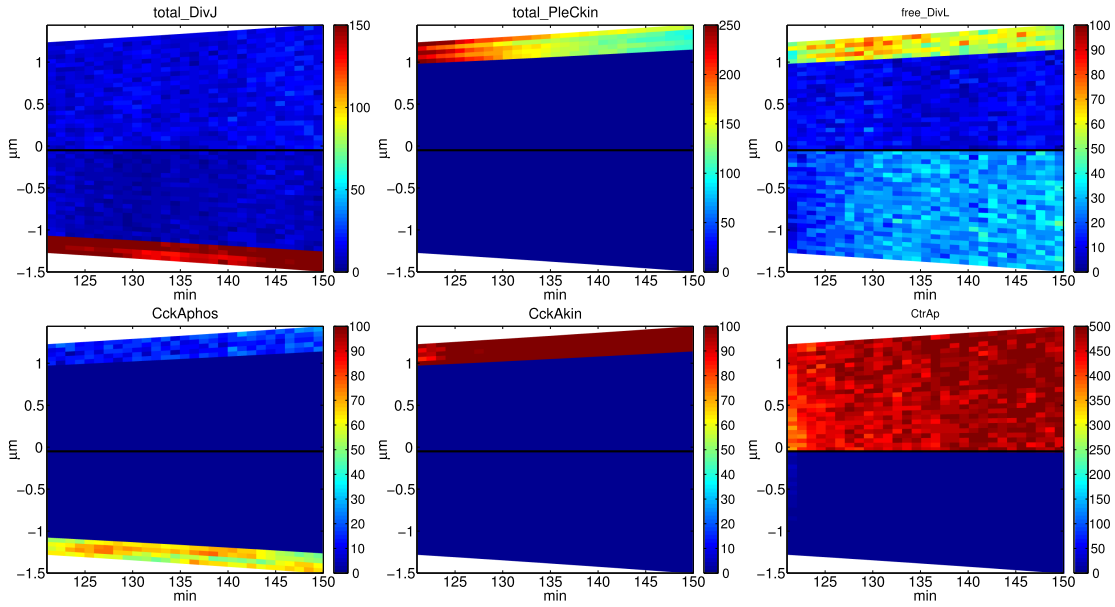

Figure 7. A typical stochastic simulation of regulatory proteins in the late predivisional stage of the *Caulobacter* cell cycle. Colors indicate the numbers of protein molecules in each bin. The bold black line marks the division plane, which separates the cell into two compartments. In the lower half (the stalked cell) DivJ is actively phosphorylating DivK, which inhibits CtrA phosphorylation. In the upper half (the nascent swarmer cell), there is insufficient DivKp to keep PleC in the kinase form. As PleC transforms to phosphatase, it dephosphorylates DivKp. Consequently, DivL is activated and CtrAp accumulates in the swarmer cell.

stage (t = 90–120 min) to the late predivisional stage (t = 120–150 min).

After 120 min, compartmentalization separates the activities of DivJ and PleC. Figure 7 shows the spatiotemporal dynamics of these proteins in the late predivsional stage. In the stalked cell, DivJ phosphorylates DivK and inhibits CtrA phosphorylation. In the swarmer cell, there is insufficient DivKp to keep PleC in the kinase form. As PleC transforms to a phosphatase, DivKp is rapidly dephosphorylated. Consequently, DivL is activated, CckA becomes a kinase, and CtrAp accumulates in the swarmer cell.

3.3. DivK overexpression negates inhibitor sequestration

In deterministic simulations, PleC at the new pole stays in the kinase form during the early predivisional stage (t = 90–120 min). PleC kinase binds to and sequesters DivKp, allowing free DivL to promote CtrA phosphorylation at the swarmer pole. Using the deterministic model, we predicted [44] that overexpression of DivK would produce enough DivKp to inhibit DivL, causing the cell cycle to block in the predivisional stage.

Our stochastic simulations are consistent, for the most part, with this ealier prediction; although, due to random fluctuations in the stochastic simulations, some cells overexpressing DivK are able to complete the cell cycle normally. Figure 8 shows representative stochastic simulations of CtrAp for cells with two-fold overexpression of DivK. Figure 9 shows a histogram of the total phosphorylated CtrA in the early predivisional stage. This simulation illustrates how randomness may affect cell fate.

In our model, the PleC phosphatase-to-kinase transition is thermodynamically more favorable when DivK is phosphorylated. However, *in vitro* experiments show that DivK need not be phosphorylated to up-regulate PleC kinase [33]. We argued that the concentration of unphosphorylated DivK *in vivo* is less than the level necessary to turn on PleC kinase activity. Therefore, DivK must first be phosphorylated by DivJ in order to activate PleC kinase functionality.

Furthermore, we predict that if DivK is sufficiently overexpressed, DivK will switch on PleC kinase activity even when DivJ is absent. As a consequence, PleC kinase further phosphorylates DivK in a positive feedback loop. DivKp then inhibits DivL and the phosphorylation of CtrA. Thus the cell is blocked in the stalked stage.

Stochastic simulations with eight-fold DivK overexpression are consistent with experiments [33] and our previous prediction. In the case of eight-fold DivK overexpression, excessive DivK binds to PleC and turns on PleC kinase activity at the new pole. Furthermore, the phosphorylated DivK inhibits CtrA phosphorylation. Therefore, the swarmer stage of the cell cycle is aborted. Figure 10 shows that, for both four-fold and eight-fold overexpression of DivK, the total population of phosphorylated CtrA molecules, on average, remains very low. Figure 11 shows histograms of the total CtrAp population at t = 30 min. For eight-fold overexpression of DivK, CtrAp levels in most cells are too low to support the swarmer stage of the cell

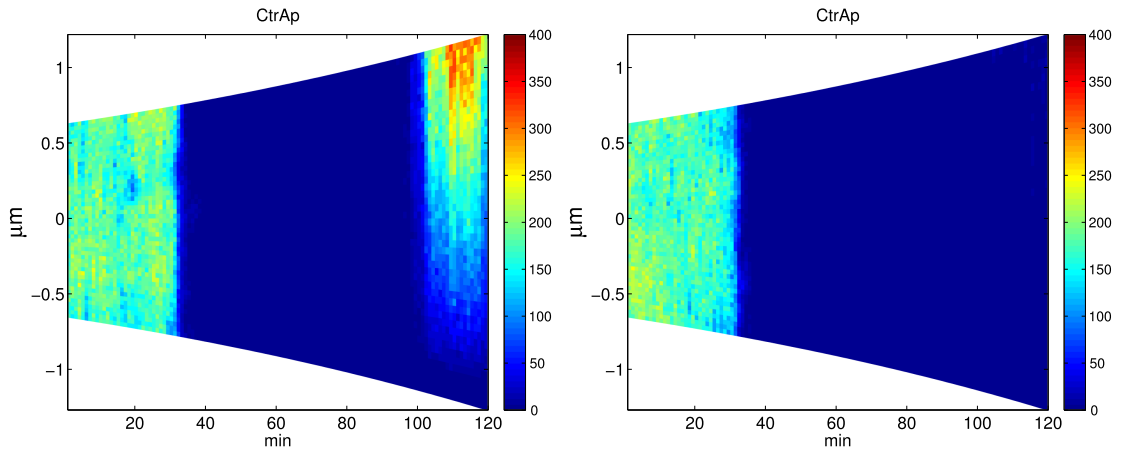

Figure 8. Representative stochastic simulations of cells that overexpress DivK two-fold. Some cells complete the cell cycle normally (left), while most cells stall in the stalked stage (right).

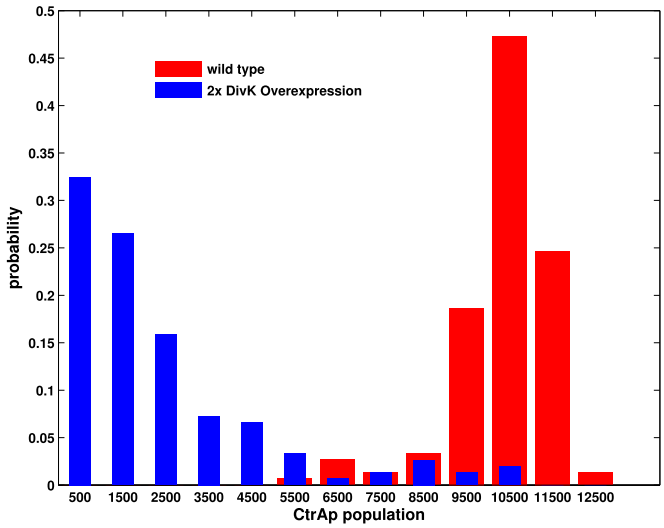

Figure 9. Histogram of total phosphorylated CtrA in the early predivisional stage. Stochastic simulations show that some cells have a high population of CtrAp, which enables them to complete the cell cycle as a wild-type cell would, while others stay in the stalk stage and fail to divide.

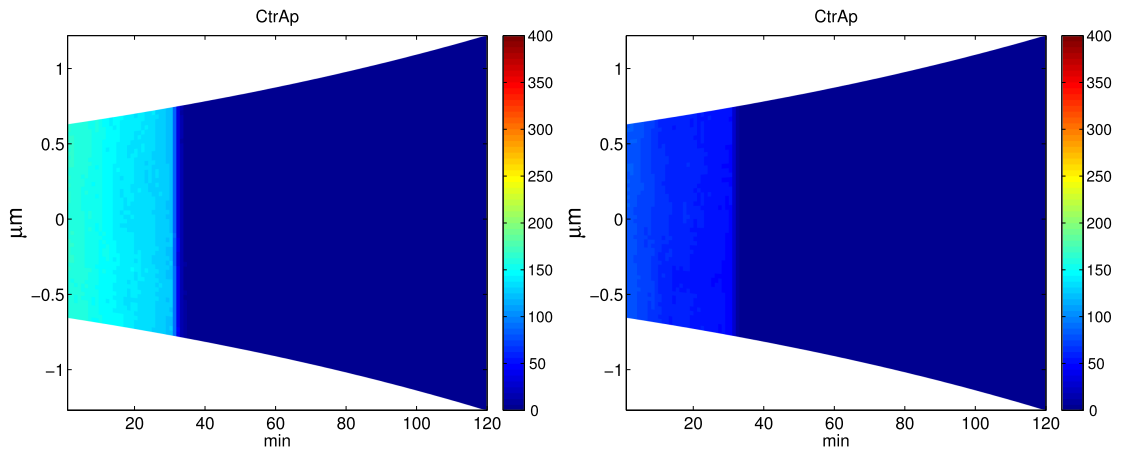

Figure 10. The average level (over 250 stochastic simulations) of total CtrAp in the case of four-fold DivK overexpression (left) and eight-fold DivK overexpression (right).

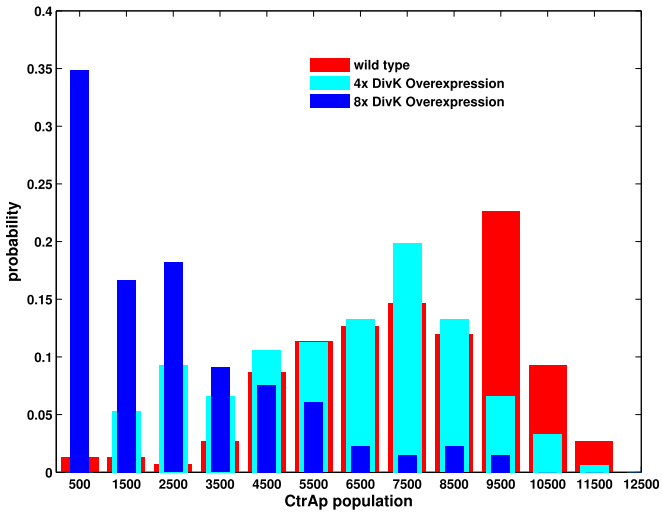

Figure 11. Histograms of CtrAp populations at $t = 30$ min. With eight-fold DivK overexpression, CtrA phosphorylation is greatly reduced in what should be the swarmer stage of the cell cycle.

cycle. For four-fold overexpression, some cells may enter the swarmer stage.

3.4. DivJ reduces the variability in swarmer-to-stalked transition time

The level of expression of *DivJ* affects both the mean and variance of cell cycle periods, as shown by the work of Lin *et al* [28]. *divJ* depletion mutants of *Caulobacter* have cell cycle periods that are slightly longer than wild-type cells and variances that are considerably larger. For stalked cells, the cell cycle period is 61 ± 7.6 min (mean $\pm$ standard deviation) for wild-type cells and 76 ± 18.7 min for *divJ* depleted cells. For swarmer cells, the values are 75 ± 7.5 min for wild-type cells and 92 ± 26 min for *divJ* depleted cells. Our goal in this subsection is to use our stochastic model to study the role of *divJ* on the regulation of noise.

To achieve this goal, we need to modify our model. In our original stochastic model, we fixed the timing of different cell cycle stages; hence, it is not suitable for studying fluctuations in cell cycle transition times. To bypass this problem, we focus in this subsection on the stage from birth of a swarmer cell to the swarmer-to-stalked transition. This is the stage when DivJ starts to accumulate and localize in the cell. First of all, we need to define a characteristic indicator for the swarmer-to-stalked transition. The output of our model is the phosphorylation state of CtrA. During the *Caulobacter* cell cycle, CtrAp level oscillates and drives the cell cycle processes required for chromosome replication, cell development and division. Figure 12 shows ten typical trajectories for oscillations of the total population of CtrAp molecules during the *Caulobacter* cell cycle. Despite stochastic fluctuations, CtrAp populations are characteristically high in the swarmer stage and drop dramatically at the swarmer-to-stalked transition. The low levels of CtrAp after the transition allow the initiation of chromosome replication.

Based on this observation, we start from the end of the swarmer cell stage ($t = 30$ min) and run stochastic simulations until the CtrAp population level drops below a threshold of 100 molecules, about 10% of the mean value of the total CtrAp population in the swarmer stage. Below this threshold, we suppose the CtrAp level is low enough to allow for chromosome replication. We define this period as the swarmer-to-stalked transition time. We also need to make changes to the model itself. In our original deterministic model [44], complete depletion of *divJ* blocks the phosphorylation of DivK, leading to high levels of free DivL, CckA kinase, and CtrAp, which inhibits the initiation of chromosome replication. These conclusions do not match with experiments [28]. To account for their experimental observations, Lin *et al* [28] proposed that other proteins may play a role similar to divJ in phosphorylating DivK. Following their lead, we modified our model to include a basal rate of phosphorylation of DivK in the absence of DivJ. With this change, figure 13 shows a histogram of swarmer-to-stalked transition times (when the total CtrAp population level drops below 100 molecules). The mean swarmer-to-stalked transition time is ~42 min in wild-type cells, and ~49 min in $\Delta divJ$ cells. Meanwhile, the standard deviation of the swarmer-to-stalked transition time increases sharply from 6 min in wild-type cells to 15 min in $\Delta divJ$ cells. These simulation results are consistent with experimental observations [28].

Besides the statistics of the swarmer-to-stalked transition time, we also plot histograms of DivKp, PleC kinase and CtrAp (figure 14) at $t = 50$ min. We can clearly see that *divJ* depleted cells have much lower levels of DivKp and PleC kinase and much higher levels of CtrAp. The wide span of CtrAp levels is

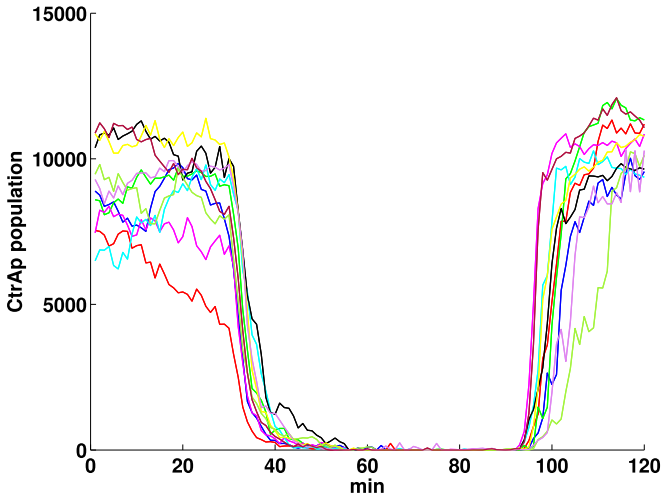

Figure 12. Typical trajectories of the total numbers of CtrAp molecules during a wild-type cell cycle. CtrAp populations are high in the swarmer stage and drop dramatically at the swarmer-to-stalked transition, to allow the initiation of chromosome replication.

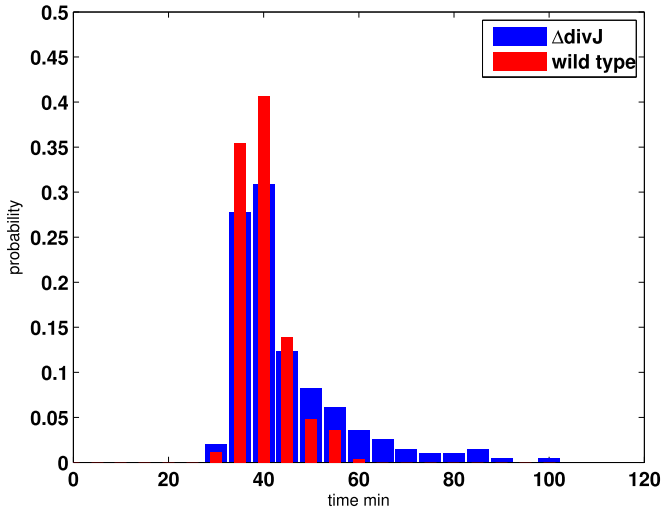

Figure 13. Histograms of swarmer-to-stalked transition times in wild-type cells and Δ*divJ* mutant cells. The mean transition time is ∼42 min for wild-type cells and ∼49 min for Δ*divJ* mutant cells. Δ*divJ* mutant cells show a much larger variance of transition times. The coefficient of variation of swarmer-to-stalked transition times is 14% for wild-type cells and 29% for Δ*divJ* cells, in very good agreement with the COVs observed by Lin *et al* [28] for total cell cycle times. We conclude that depletion of *divJ* doesn't stall the swarmer-to-stalked transition for long, but it causes large fluctuations in the transition time.

another indication of the larger variance of the swarmer-to-stalked transition time.

4. Discussion and conclusion

In earlier work [44], we proposed a mathematical model of a bistable PleC switch, for which the PleC phosphatase-to-kinase transition is flipped by DivJ. In this paper we present a stochastic model of the spatiotemporal regulation of the histidine kinase phosphorelay mechanism in *Caulobacter crescentus*. In this model, we show that inhibitor sequestration is an important function of the bifunctional histidine kinase PleC [44]. Our simulation results show that, in the early predivisional stage, the binding of DivKp to PleC kinase at the new pole may prevent DivKp from binding to DivL and inhibiting DivL's role in activating CckA kinase. Furthermore, stochastic simulations of *divK*-overexpressing cells confirm that excessive DivKp can inhibit DivL at the new pole, thereby inhibiting CtrA phosphorylation and swarmer cell development.

In addition, we use our stochastic model (suitably modified) to study variability in the time it takes a newborn swarmer cell to dephosphorylate CtrAp and initiate a new round of DNA synthesis. This transition is sensitively dependent on the kinase DivJ, which initiates a sequence of events leading to CtrAp dephosphorylation. Consequently, deletion of the *divJ* gene lengthens the time needed for dephosphorylation of CtrAp and completion of the swarmer-to-stalked transition. Moreover, *divJ* deletion causes unusually

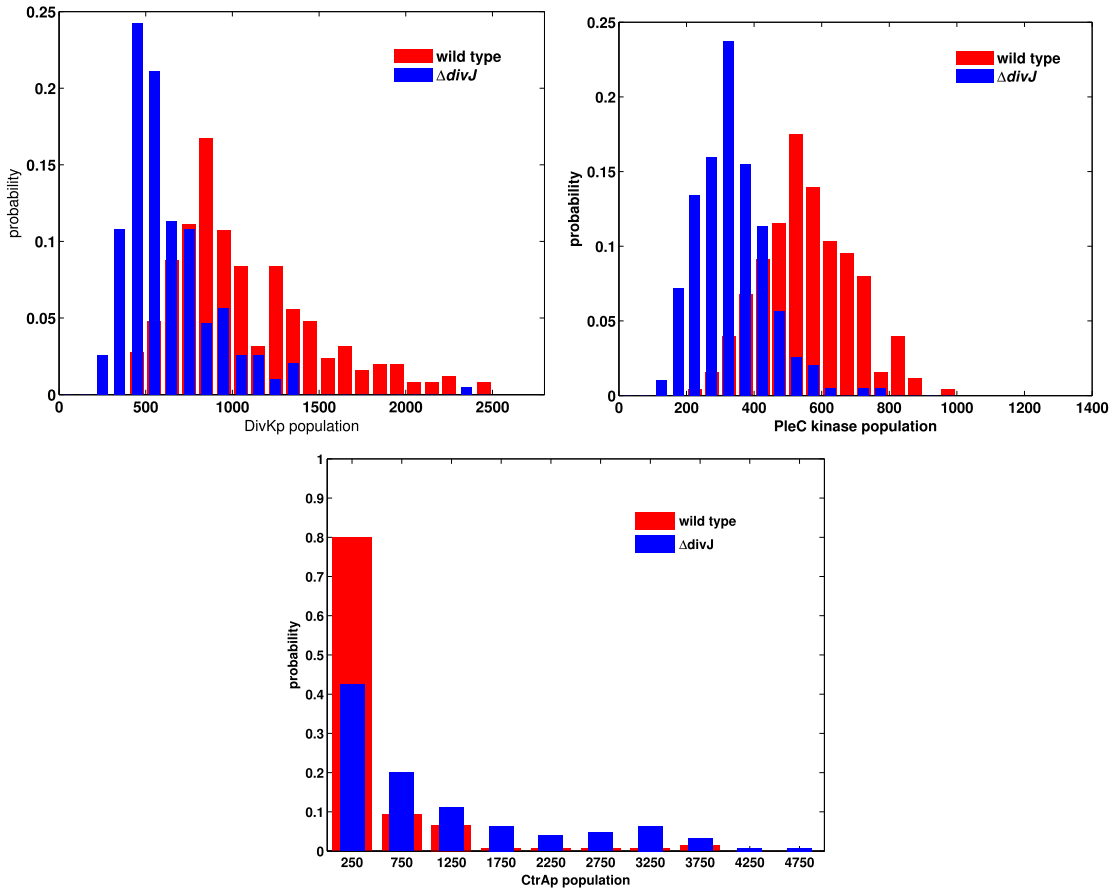

Figure 14. Histograms of DivKp, PleC kinase and CtrAp at $t = 50$ min in wild-type and $\Delta divJ$ cells.

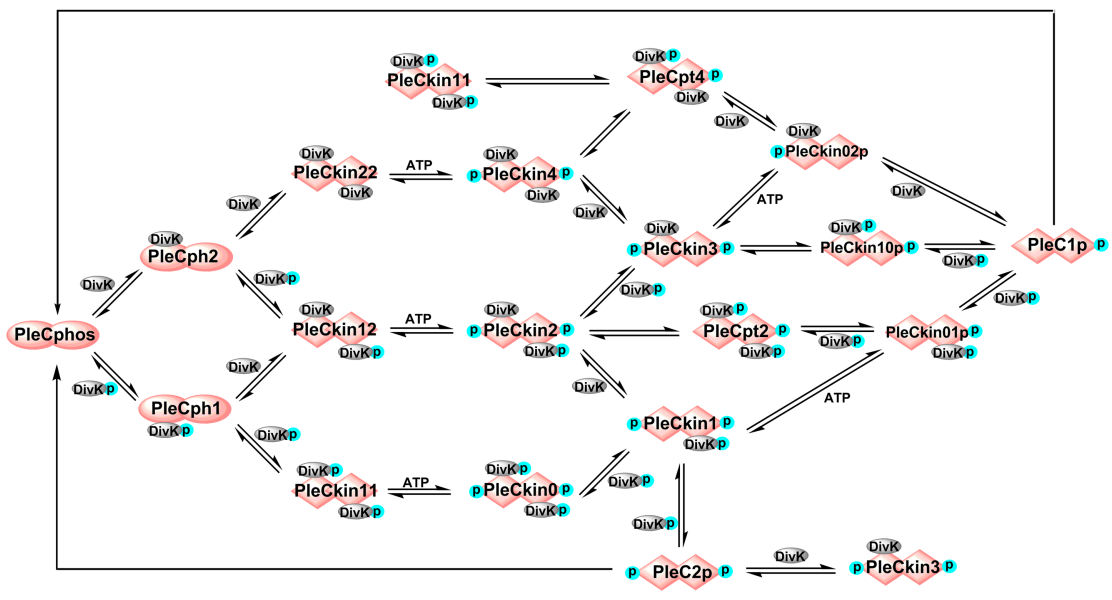

Figure A1. The transformations of PleC kinase and phosphatase when interacting with DivK and DivKp.

large fluctuations in time needed to execute the swarmer-to-stalked transition, as is observed experimentally [28].

Although our spatiotemporal stochastic model successfully accounts for certain aspects of the *Caulobacter* cell cycle, our model is still very incomplete. We have focussed only on the dynamics of the PleC- and CckA-phosphorelay systems. Many other important regulators of the *Caulobacter* cell cycle have been ignored or highly abstracted . For instance, we

Table A1. Chemical reactions and propensity calculation.

Reaction	Rate Const.	Propensity
$\varnothing \xrightarrow{divJ} \mathrm{mRNA_{DivJ}}$	$ks_{rna} = 0.625$	$a = ks_{rna} \cdot divJ$
$\mathrm{mRNA_{DivJ}} \rightarrow \varnothing$	$kd_{rna} = 0.25$	$a = kd_{rna} \cdot mRNA_{DivJ}$
$\varnothing \xrightarrow{divK} \mathrm{mRNA_{DivK}}$	$ks_{rna} = 0.625$	$a = ks_{rna} \cdot divK$
$\mathrm{mRNA_{DivK}} \rightarrow \varnothing$	$kd_{rna} = 0.25$	$a = kd_{rna} \cdot mRNA_{DivK}$
$\varnothing \xrightarrow{pleC} \mathrm{mRNA_{PleC}}$	$ks_{rna} = 0.625$	$a = ks_{rna} \cdot pleC$
$\mathrm{mRNA_{PleC}} \rightarrow \varnothing$	$kd_{rna} = 0.25$	$a = kd_{rna} \cdot mRNA_{PleC}$
$\varnothing \xrightarrow{divL} \mathrm{mRNA_{DivL}}$	$ks_{rna} = 0.625$	$a = ks_{rna} \cdot divL$
$\mathrm{mRNA_{DivL}} \rightarrow \varnothing$	$deg_{rna} = 0.25$	$a = kd_{rna} \cdot mRNA_{DivL}$
$\varnothing \xrightarrow{cckA} \mathrm{mRNA_{CckA}}$	$ks_{rna} = 0.625$	$a = ks_{rna} \cdot cckA$
$\mathrm{mRNA_{CckA}} \rightarrow \varnothing$	$kd_{rna} = 0.25$	$a = kd_{rna} \cdot mRNA_{CckA}$
$\varnothing \xrightarrow{ctrA} \mathrm{mRNA_{CtrA}}$	$ks_{rna} = 0.625$	$a = ks_{rna} \cdot ctrA$
$\mathrm{mRNA_{CtrA}} \rightarrow \varnothing$	$kd_{rna} = 0.25$	$a = kd_{rna} \cdot mRNA_{CtrA}$
$\varnothing \xrightarrow{\mathrm{mRNA_{DivK}}} \mathrm{DivK}$	$ks_{dk} = 25.0$	$a = ks_{dk} \cdot mRNA_{DivK}$
$\mathrm{DivK} \rightarrow \varnothing$	$kd_{DivK} = 0.005$	$a = kd_{DivK} \cdot DivK$
$\mathrm{DivKp} \rightarrow \varnothing$	$kd_{DivKp} = 0.005$	$a = kd_{DivKp} \cdot DivKp$
$\varnothing \xrightarrow{\mathrm{mRNA_{PleC}}} \mathrm{PleC^f}$	$ks_{PleC} = 50.0$	$a = ks_{PleC} \cdot mRNA_{PleC}$
$\mathrm{PleC^f} \rightarrow \varnothing$	$kd_{PleC} = 0.05$	$a = kd_{PleC} \cdot PleC^f$
$\mathrm{PleC^f} \rightarrow \mathrm{PleCphos}$	$kb_{pc} = 1.0$	$a = kb_{pc} \cdot PleC^f$
$\mathrm{PleCphos} \rightarrow \mathrm{PleC^f}$	$kub_{pc} = 0.5$	$a = kub_{pc} \cdot PleCphos$
$\mathrm{PleCphos + DivKp} \rightarrow \mathrm{PleCph1}$	$kb_{kp:phos} = 5.0$	$a = kb_{kp:phos}/(h \cdot S) \cdot PleCphos \cdot DivKp$
$\mathrm{PleCphos + DivK} \rightarrow \mathrm{PleCph2}$	$kb_{k:phos} = 0.05$	$a = kb_{k:phos}/(h \cdot S) \cdot PleCphos \cdot DivK$
$\mathrm{PleCph1} \rightarrow \mathrm{PleCphos + DivKp}$	$kub_{ph1:kp} = 5.0$	$a = kub_{ph1:kp} \cdot PleCph1$
$\mathrm{PleCph2} \rightarrow \mathrm{PleCphos + DivK}$	$kub_{ph2:k} = 5.0$	$a = kub_{ph2:k} \cdot PleCph2$
$\mathrm{PleCph2} \rightarrow \mathrm{PleCph1}$	$kph_{ph2} = 0.005$	$a = kph_{ph2} \cdot PleCph2$
$\mathrm{PleCph1} \rightarrow \mathrm{PleCph2}$	$kdp_{ph1} = 10.0$	$a = kdp_{ph1} \cdot PleCph1$
$\mathrm{PleCph1 + DivK} \rightarrow \mathrm{PleCph2 + DivKp}$	$kb_{k:ph} = 0.016$	$a = kb_{k:ph}/(h \cdot S) \cdot PleCph1 \cdot DivK$
$\mathrm{PleCph2 + DivKp} \rightarrow \mathrm{PleCph1 + DivK}$	$kb_{kp:ph} = 1.6$	$a = kb_{kp:ph}/(h \cdot S) \cdot PleCph2 \cdot DivKp$
$\mathrm{PleCph1 + DivKp} \rightarrow \mathrm{PleCkin11}$	$kb_{kp:ph1} = 5.0$	$a = kb_{kp:ph1}/(h \cdot S) \cdot PleCph1 \cdot DivKp$
$\mathrm{PleCph1 + DivK} \rightarrow \mathrm{PleCkin12}$	$kb_{k:ph} = 0.016$	$a = kb_{k:ph}/(h \cdot S) \cdot PleCph1 \cdot DivK$
$\mathrm{PleCph2 + Di\text{-}vKp} \rightarrow \mathrm{PleCkin12}$	$kb_{kp:ph} = 1.6$	$a = kb_{kp:ph}/(h \cdot S) \cdot PleCph2 \cdot DivKp$
$\mathrm{PleCph2 + DivK} \rightarrow \mathrm{PleCkin22}$	$kb_{k:ph} = 0.016$	$a = kb_{k:ph}/(h \cdot S) \cdot PleCph2 \cdot DivK$
$\mathrm{PleCkin11} \rightarrow \mathrm{PleCph1 + DivKp}$	$kub_{kp:kin11} = 2.5$	$a = kub_{kp:kin11} \cdot PleCkin11$
$\mathrm{PleCkin12} \rightarrow \mathrm{PleCph2 + DivKp}$	$kub_{kp:kin12} = 1.6e-4$	$a = kub_{kp:kin12} \cdot PleCkin12$
$\mathrm{PleCkin12} \rightarrow \mathrm{PleCph1 + DivK}$	$kub_{k:kin12} = 1.6e-4$	$a = kub_{k:kin12} \cdot PleCkin12$
$\mathrm{PleCkin22} \rightarrow \mathrm{PleCph2 + DivK}$	$kub_{k:kin22} = 1.6e-8$	$a = kub_{k:kin22} \cdot PleC22$
$\mathrm{PleCkin11} \rightarrow \mathrm{PleCkin0}$	$kph_{kin11} = 2.5$	$a = kph_{kin11} \cdot PleCkin11$
$\mathrm{PleCkin12} \rightarrow \mathrm{PleCkin2}$	$k_{phos} = 5.0$	$a = k_{phos} \cdot PleCkin12$
$\mathrm{PleCkin22} \rightarrow \mathrm{PleCkin4}$	$k_{phos} = 5.0$	$a = k_{phos} \cdot PleCkin22$
$\mathrm{PleCkin0} \rightarrow \mathrm{PleCkin11}$	$k_{deph} = 5.0$	$a = k_{deph} \cdot PleCkin0$
$\mathrm{PleCkin2} \rightarrow \mathrm{PleCkin12}$	$k_{deph} = 5.0$	$a = k_{deph} \cdot PleCkin2$
$\mathrm{PleCkin4} \rightarrow \mathrm{PleCkin22}$	$k_{deph} = 5.0$	$a = k_{deph} \cdot PleCkin4$
$\mathrm{PleCkin0} \rightarrow \mathrm{PleCkin1 + DivKp}$	$kub_{kp:pc} = 0.16$	$a = kub_{kp:pc} \cdot PleCkin0$
$\mathrm{PleCkin2} \rightarrow \mathrm{PleCkin3 + DivKp}$	$kub_{kp:pc} = 0.16$	$a = kub_{kp:pc} \cdot PleCkin2$
$\mathrm{PleCkin2} \rightarrow \mathrm{PleCkin1 + DivK}$	$kub_{k:pc} = 1.6e-3$	$a = kub_{k:pc} \cdot PleCkin2$
$\mathrm{PleCkin4} \rightarrow \mathrm{PleCkin3 + DivK}$	$kub_{k:pc} = 1.6e-3$	$a = kub_{k:pc} \cdot PleCkin4$
$\mathrm{PleCkin1 + DivKp} \rightarrow \mathrm{PleCkin0}$	$kb_{kp:pc} = 5.0$	$a = kb_{kp:pc}/(h \cdot S) \cdot PleCkin1 \cdot DivKp$
$\mathrm{PleCkin1 + DivK} \rightarrow \mathrm{PleCkin2}$	$kb_{k:pc} = 5.0$	$a = kb_{k:pc}/(h \cdot S) \cdot PleCkin1 \cdot DivK$
$\mathrm{PleCkin3 + DivKp} \rightarrow \mathrm{PleCkin2}$	$kb_{kp:pc} = 5.0$	$a = kb_{kp:pc}/(h \cdot S) \cdot PleCkin3 \cdot DivKp$
$\mathrm{PleCkin3 + DivK} \rightarrow \mathrm{PleCkin4}$	$kb_{k:pc} = 5.0$	$a = kb_{k:pc}/(h \cdot S) \cdot PleCkin3 \cdot DivK$
$\mathrm{PleCkin1} \rightarrow \mathrm{PleC2p + DivKp}$	$kub_{kp:pc} = 0.16$	$a = kub_{kp:pc} \cdot PleCkin1$
$\mathrm{PleCkin3} \rightarrow \mathrm{PleC2p + DivK}$	$kub_{k:pc} = 1.6e-3$	$a = kub_{k:pc} \cdot PleCkin3$
$\mathrm{PleC2p + DivKp} \rightarrow \mathrm{PleCkin1}$	$kb_{kp:pc} = 5.0$	$a = kb_{kp:pc}/(h \cdot S) \cdot PleC2p \cdot DivKp$
$\mathrm{PleC2p + DivK} \rightarrow \mathrm{PleCkin3}$	$kb_{k:pc} = 5.0$	$a = kb_{k:pc}/(h \cdot S) \cdot PleC2p \cdot DivK$
$\mathrm{PleC2p} \rightarrow \mathrm{PleCphos}$	$k_{deph} = 5.0$	$a = kdeph \cdot PleC2p$
$\mathrm{PleCkin10p} \rightarrow \mathrm{PleC1p + DivKp}$	$kub_{kp:pc} = 0.16$	$a = kub_{kp:pc} \cdot PleCkin10p$
$\mathrm{PleCkin01p} \rightarrow \mathrm{PleC1p + DivKp}$	$kub_{kp:pc} = 0.16$	$a = kub_{kp:pc} \cdot PleCkin01p$
$\mathrm{PleCkin02p} \rightarrow \mathrm{PleC1p + DivK}$	$kub_{k:pc} = 1.6e-3$	$a = kub_{k:pc} \cdot PleCkin02p$

Table A1. (Continued.)

Reaction	Rate Const.	Propensity
PleC1p + DivKp → PleCkin10p	$kb_{kp:pc} = 5.0$	$a = kb_{kp:pc}/(h \cdot S) \cdot PleC1p \cdot DivKp$
PleC1p + DivKp → PleCkin01p	$kb_{kp:pc} = 5.0$	$a = kb_{kp:pc}/(h \cdot S) \cdot PleC1p \cdot DivKp$
PleC1p + DivK → PleCkin02p	$kb_{k:pc} = 5.0$	$a = kb_{k:pc}/(h \cdot S) \cdot PleC1p \cdot DivK$
PleC1p → PleCphos	$k_{deph} = 5.0$	$a = k_{deph} \cdot PleC1p$
PleCkin3 → PleCkin10p	$k_{auto} = 5.0$	$a = k_{auto} \cdot PleCkin3$
PleCkin2 → PleCpt2	$k_{auto} = 5.0$	$a = k_{auto} \cdot PleCkin2$
PleCkin4 → PleCpt4	$k_{auto} = 5.0$	$a = k_{auto} \cdot PleCkin4$
PleCpt4 → PleCkin11	$k_{auto} = 5.0$	$a = k_{auto} \cdot PleCpt4$
PleCkin10p → PleCkin3	$k_{dauto} = 0.16$	$a = k_{dauto} \cdot PleCkin10p$
PleCpt2 → PleCkin2	$k_{dauto} = 0.16$	$a = k_{dauto} \cdot PleCpt2$
PleCpt4 → PleCkin4	$k_{dauto} = 0.16$	$a = k_{dauto} \cdot PleCpt4$
PleCkin11 → PleCpt4	$k_{dp:kin11} = 0.0755$	$a = k_{dp:kin11} \cdot PleCkin11$
PleCkin1 → PleCkin01p	$k_{deph} = 5.0$	$a = k_{deph} \cdot PleCkin1$
PleCkin3 → PleCkin02p	$k_{deph} = 5.0$	$a = k_{deph} \cdot PleCkin3$
PleCkin01p → PleCkin1	$k_{phos} = 5.0$	$a = k_{phos} \cdot PleCkin01p$
PleCkin02p → PleCkin3	$k_{phos} = 5.0$	$a = k_{phos} \cdot PleCkin02p$
PleCkin01p + DivKp → PleCpt2	$kb_{kp:pc} = 5.0$	$a = kb_{kp:pc}/(h \cdot S) \cdot PleCkin01p \cdot DivKp$
PleCkin02p + DivKp → PleCpt4	$kb_{kp:pc} = 5.0$	$a = kb_{kp:pc}/(h \cdot S) \cdot PleCkin02p \cdot DivKp$
PleCpt2 → PleCkin01p + DivKp	$kub_{kp:pc} = 0.16$	$a = kub_{kp:pc} \cdot PleCpt2$
PleCpt4 → PleCkin02p + DivKp	$kub_{kp:pc} = 0.16$	$a = kub_{kp:pc} \cdot PleCpt4$
PleCphos →∅	$kd_{PleC} = 0.05$	$a = kd_{PleC} \cdot PleCphos$
PleCph1 → DivKp	$kd_{PleC} = 0.05$	$a = kd_{PleC} \cdot PleCph1$
PleCph2 →∅	$kd_{PleC} = 0.05$	$a = kd_{PleC} \cdot PleCph2$
PleCkin11 → DivKp + DivKp	$kd_{PleC} = 0.05$	$a = kd_{PleC} \cdot PleCkin11$
PleCkin12 → DivKp	$kd_{PleC} = 0.05$	$a = kd_{PleC} \cdot PleCkin12$
PleCkin22 →∅	$kd_{PleC} = 0.05$	$a = kd_{PleC} \cdot PleCkin22$
PleCkin0 → DivKp + DivKp	$kd_{PleC} = 0.05$	$a = kd_{PleC} \cdot PleCkin0$
PleCkin2 → DivKp	$kd_{PleC} = 0.05$	$a = kd_{PleC} \cdot PleCkin2$
PleCkin4 →∅	$kd_{PleC} = 0.05$	$a = kd_{PleC} \cdot PleCkin4$
PleCkin1 → DivKp	$kd_{PleC} = 0.05$	$a = kd_{PleC} \cdot PleCkin1$
PleCkin3 →∅	$kd_{PleC} = 0.05$	$a = kd_{PleC} \cdot PleCkin3$
PleC2p →∅	$kd_{PleC} = 0.05$	$a = kd_{PleC} \cdot PleC2p$
PleC1p →∅	$kd_{PleC} = 0.05$	$a = kd_{PleC} \cdot PleC1p$
PleCkin02p →∅	$kd_{PlC} = 0.05$	$a = kd_{PleC} \cdot PleCkin02p$
PleCkin10p → DivKp	$kd_{PleC} = 0.05$	$a = kd_{PleC} \cdot PleCkin10p$
PleCkin01p → DivKp	$kd_{PleC} = 0.05$	$a = kd_{PleC} \cdot PleCkin01p$
PleCpt4 → DivKp	$kd_{PleC} = 0.05$	$a = kd_{PleC} \cdot PleCpt4$
PleCpt2 → DivKp + DivKp	$kd_{PleC} = 0.05$	$a = kd_{PleC} \cdot PleCpt2$
$\varnothing \xrightarrow{\text{mRNA}_{\text{DivJ}}} \text{DivJ}^{\text{f}}$	$ks_{DivJ} = 12.5$	$a = ks_{DivJ} \cdot mRNA_{DivJ}$
$\text{DivJ}^{\text{f}} \rightarrow \varnothing$	$kd_{DivJ} = 0.05$	$a = kd_{DivJ} \cdot DivJ^{f}$
$\text{DivJ}^{\text{f}} \rightarrow$ DivJ	$kb_{dj} = 1.0$	$a = kb_{dj} \cdot DivJ^{f}$
DivJ → ∅	$kd_{DivJ} = 0.05$	$a = kd_{DivJ} \cdot DivJ$
DivJ + DivK → DivJK	$kb_{k:dj} = 5.0$	$a = kb_{k:dj}/(h \cdot S) \cdot DivJ \cdot DivK$
DivJK → DivJ + DivK	$kub_{k:jk} = 0.0016$	$a = kub_{k:jk} \cdot DivJK$
DivJK → DivJKp	$kph_{jk} = 5.0$	$a = kph_{jk} \cdot DivJK$
DivJKp → DivJK	$kdph_{jkp} = 0.16$	$a = kdph_{jkp} \cdot DivJKp$
DivJKp → DivJ + DivKp	$kub_{kp:jkp} = 1.0$	$a = kub_{kp:jkp} \cdot DivJKp$
DivJ + DivKp → DivJKp	$kbd_{kp:j} = 5.0$	$a = kbd_{kp:j}/(h \cdot S) \cdot DivJ \cdot DivKp$
DivJK →∅	$kd_{jk} = 0.05$	$a = kd_{DivJ} \cdot DivJK$
DivJKp →∅	$kd_{jkp} = 0.05$	$a = kd_{DivJ} \cdot DivJKp$
DivK → DivKp	$kph_{dk} = 0.05$	$a = kph_{dk} \cdot DivK$
DivKp → DivK	$kdph_{kp} = 0.01$	$a = kdph_{kp} \cdot DivKp$
$\varnothing \xrightarrow{\text{mRNA}_{\text{DivL}}} \text{DivL}^{\text{f}}$	$ks_{DivL} = 12.5$	$a = ks_{DivL} \cdot mRNA_{DivL}$
$\text{DivL}^{\text{f}} \rightarrow \varnothing$	$kd_{DivL} = 0.05$	$a = kd_{DivL} \cdot DivL^{f}$
$\text{DivL}^{\text{f}} \rightarrow$ DivL	$kb_{DivL} = 1.0$	$a = kb_{DivL} \cdot DivL^{f}$
DivL → DivL^{f}	$kub_{DivL} = 0.1$	$a = kub_{DivL} \cdot DivL$
DivL → ∅	$kd_{DivL} = 0.05$	$a = kd_{DivL} \cdot DivL$
DivL + DivKp → DivLKp	$kb_{kp:dl} = 2.5$	$a = kb_{kp:dl}/(h \cdot S) \cdot DivL \cdot DivKp$
DivLKp → DivL + DivKp	$kub_{kp:lkp} = 0.5$	$a = kub_{kp:lkp} \cdot DivLKp$

Table A1. (Continued.)

Reaction	Rate Const.	Propensity
$\mathrm{DivLKp} \rightarrow \varnothing$	$kd_{DivL} = 0.05$	$a = kd_{DivL} \cdot DivLKp$
$\varnothing \xrightarrow{\mathrm{mRNA_{CckA}}} \mathrm{CckA^f}$	$ks_{CckA} = 12.5$	$a = ks_{CckA} \cdot mRNA_{CckA}$
$\mathrm{CckA^f} \rightarrow \varnothing$	$kd_{CckA} = 0.05$	$a = kd_{CckA} \cdot CckA^f$
$\mathrm{CckA^f} \rightarrow \mathrm{CckAphos}$	$kb_{CckA} = 1.0$	$a = kb_{CckA} \cdot CckA^f$
$\mathrm{CckAphos} \rightarrow \mathrm{CckA^f}$	$kub_{CckA} = 0.1$	$a = kub_{CckA} \cdot CckAphos$
$\mathrm{CckAphos} \xrightarrow{\mathrm{DivL}} \mathrm{CckAkin}$	$k_{ck} = 10.0, K_m = 0.5$	$a = k_{ck} \frac{DivL^4}{DivL^4 + (K_m \cdot h \cdot S)^4}$
$\mathrm{CckAkin} \rightarrow \mathrm{CckAphos}$	$k_{ph:ck} = 1.0$	$a = k_{ph:ck} \cdot CckAkin$
$\mathrm{CckAkin} \rightarrow \varnothing$	$kd_{CckA} = 0.05$	$a = kd_{CckA} \cdot CckAkin$
$\mathrm{CckAphos} \rightarrow \varnothing$	$kd_{CckA} = 0.05$	$a = kd_{CckA} \cdot CckAphos$
$\varnothing \xrightarrow{\mathrm{mRNA_{CtrA}}} \mathrm{CtrA}$	$ks_{CtrA} = 25.0$	$a = ks_{CtrA} \cdot mRNA_{CtrA}$
$\mathrm{CtrA} \rightarrow \varnothing$	$kd_{CtrA} = 0.05$	$a = kph_{CtrA} \cdot CtrA$
$\mathrm{CtrAp} \rightarrow \varnothing$	$kd_{CtrA} = 0.05$	$a = kdph_{CtrAp} \cdot CtrAp$
$\mathrm{CtrA} \xrightarrow{\mathrm{CckAkin}} \mathrm{CtrAp}$	$kph_{CtrA} = 600.0$	$a = kd_{CtrA}/(h \cdot S) \cdot CtrA \cdot CckAkin$
$\mathrm{CtrAp} \xrightarrow{\mathrm{CckAphos}} \mathrm{CtrA}$	$kdph_{CtrAp} = 600.0$	$a = kd_{CtrA}/(h \cdot S) \cdot CtrAp \cdot CckAphos$

Table A2. Diffusion steps and propensity calculation

Diffusive Jump	Rate Const.	Propensity
$\mathrm{DivJ_i^f} \rightarrow \mathrm{DivJ_{i+1}^f}$	$D_{dj} = 10.0$	$a = D_{dj}/h^2 \cdot DivJ_i^f$
$\mathrm{DivJ_i^f} \rightarrow \mathrm{DivJ_{i-1}^f}$	$D_{dj} = 10.0$	$a = D_{dj}/h^2 \cdot DivJ_i^f$
$\mathrm{PleC^{f_i \rightarrow PleC_i^f + 1}}$	$D_{pc} = 10.0$	$a = D_{pc}/h^2 \cdot PleC_i^f$
$\mathrm{PleC_i^f} \rightarrow \mathrm{PleC_{i-1}^f}$	$D_{pc} = 10.0$	$a = D_{pc}/h^2 \cdot PleC_i^f$
$\mathrm{DivK_i} \rightarrow \mathrm{DivK_{i+1}}$	$D_{dk} = 10.0$	$a = D_{dk}/h^2 \cdot DivK_i$
$\mathrm{DivK_i} \rightarrow \mathrm{DivK_{i-1}}$	$D_{dk} = 10.0$	$a = D_{dk}/h^2 \cdot DivK_i$
$\mathrm{DivKp_i} \rightarrow \mathrm{DivKp_{i+1}}$	$D_{dk} = 10.0$	$a = D_{dk}/h^2 \cdot DivKp_i$
$\mathrm{DivKp_i} \rightarrow \mathrm{DivKp_{i-1}}$	$D_{dk} = 10.0$	$a = D_{dk}/h^2 \cdot DivKp_i$
$\mathrm{DivL_i^f} \rightarrow \mathrm{DivL_{i+1}^f}$	$D_{dl} = 10.0$	$a = D_{dl}/h^2 \cdot DivL_i^f$
$\mathrm{DivL_i^f} \rightarrow \mathrm{DivL_{i-1}^f}$	$D_{dl} = 10.0$	$a = D_{dl}/h^2 \cdot DivL_i^f$
$\mathrm{CckA_i^f} \rightarrow \mathrm{CckA_{i+1}^f}$	$D_{ck} = 10.0$	$a = D_{ck}/h^2 \cdot CckA_i^f$
$\mathrm{CckA_i^f} \rightarrow \mathrm{CckA_{i-1}^f}$	$D_{ck} = 10.0$	$a = D_{ck}/h^2 \cdot CckA_i^f$
$\mathrm{CtrA_i} \rightarrow \mathrm{CtrA_{i+1}}$	$D_{ca} = 10.0$	$a = D_{ca}/h^2 \cdot CtrA_i$
$\mathrm{CtrA_i} \rightarrow \mathrm{CtrA_{i-1}}$	$D_{ca} = 10.0$	$a = D_{ca}/h^2 \cdot CtrA_i$
$\mathrm{CtrAp_i} \rightarrow \mathrm{CtrAp_{i+1}}$	$D_{ca} = 10.0$	$a = D_{ca}/h^2 \cdot CtrAp_i$
$\mathrm{CtrAp_i} \rightarrow \mathrm{CtrAp_{i-1}}$	$D_{ca} = 10.0$	$a = D_{ca}/h^2 \cdot CtrAp_i$

have ignored (for the time being) the important roles played by proteins such as PopZ, GcrA, FtsZ and ClpXP, and we have enforced the spatial localization of DivJ, PleC, DivL and CckA by setting spatial 'localization indicators' to 0 or 1 at specific stages of the cell cycle (see 'model details' and figure A2 in the appendix). These assumptions, which have served our purposes in this paper, will have to be lifted in future editions of the model. In the future, we will also extend our one-dimensional (1D) model of a cylindrical *Caulobacter* cell to a more realistic 2D model of a banana-shaped cell. Stochastic simulations on a 2D domain may lead to significantly different results, based on previous research results [19, 20].

Acknowledgments

This work was supported by the National Science Foundation under awards DMS-1225160, CCF-0953590, and CCF-1526666.

Appendix. Model details

For *Caulobacter*, we model the banana shaped cell with a 1D domain along its long axis and discretize the corresponding 1D reaction–diffusion system into 50 compartments ('bins'), as in the RDME framework. In each compartment, all chemical reactions (listed in table A1) as well as all diffusive jumps (listed in table A2) are simulated by 'direct method' of SSA.

When a *Caulobacter* cell grows, new cell wall material is synthesized uniformly along the long axis. Thus, we assume that during *Caulobacter* cell cycle, the length of each compartment grows exponentially in time as

$$\frac{\mathrm{d}h}{\mathrm{d}t} = \mu \cdot h. \tag{2}$$

The new born swarmer cell of *Caulobacter* has a length of 1.3 μm. Over the next 150 min the cell grows to 3.0 μm before cell division. Therefore, we can calculate the growth rate as $\mu = 0.0055\ \mathrm{min}^{-1}$.

The deterministic model [44] uses dimensionless variables for all protein concentrations. Therefore, to convert the dimensionless ODEs of the deterministic model to discrete population variables suitable for simulation by Gillespie's SSA, we must convert dimensionless concentration variables into numbers of protein molecules per cell. Based on accepted biological numbers [31], we choose the conversion factor $S = 1000$ molecules per unit concentration. After scaling the variables in this way, we must also make adjustments to the second-order rate constants in the model. In addition, the conversion of the Hill function in the stochastic model needs special attention. To maintain the sigmoidal character of the Hill function, we average [27] the populations of *divL* molecules over five neighboring bins before calculating the propensity of the reaction.

Before DNA replication starts, there is only one copy of the bacterial chromosome, with its origin of replication near the old pole. In our simulation, we locate the original copy of the chromosome within

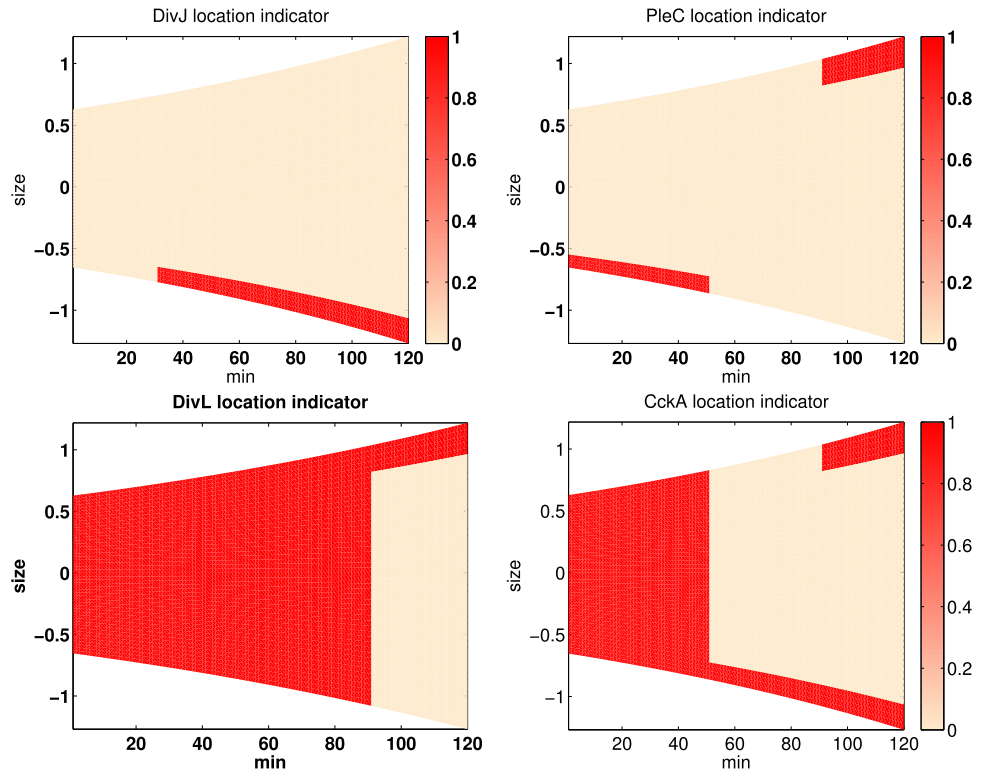

Figure A2. Localization indicators for DivJ (upper left), PleC (upper right), DivL (lower left) and CckA (lower right). The indicator functions = 0 (yellow) or 1 (red).

20% of the cell length from the old pole i.e. 10 bins from the old pole. Hence all mRNA molecules are transcribed from the original chromosome only in this region. By $t = 50$ min, when chromosome replication and segregation are complete, a second copy of the chromosome is introduced near the new pole (within 20% of the length to the new pole). All mRNA molecules are transcribed from the second chromosome only in this region as well. Experiments [4, 50] show that there exists only ~ 3 mRNA molecules per cell on average for each gene, and these mRNAs can be short lived (half life ~3 min). Based on these estimates, we select the rate constants for mRNA synthesis and degradation to be $k_{\text{syn\_mRNA}} = 0.626\ \text{min}^{-1}$ and $k_{\text{deg\_mRNA}} = 0.25\ \text{min}^{-1}$.

Moreover, because the mechanisms for localization of DivJ, PleC, DivL and CckA are not yet very well understood, we deliberately enforce their localization in specific places at specific times in the cell cycle, based on experimental observations in wild-type and mutant cells. The scheme for localizing species S to the ith compartment is given by

$$S_i^f \xrightarrow[\text{localization\_indicator}]{kb} S_i.$$

The free form of species S^f is synthesized at the location of its mRNA message and subsequently diffuses freely within the cell. When the localization indicator is set = 1 at certain positions, species S becomes bound to those positions, according to the above reaction. When the localization indicator is set = 0, the species is released from the position. Figure A2 illustrates the localization indicator settings for the four proteins at different stages of the cell cycle. In the swarmer stage, PleC is localized at the old pole. At the beginning of the swarmer-to-stalked transition (t = 30 min), DivJ localizes to the old pole. After a short colocalization with DivJ, PleC is cleared from the old pole (t = 50–90 min) and relocates to the new pole in the early predivisional stage (t = 90–120 min). In the swarmer stage (t = 0–30 min) and during the swarmer-to-stalked transition (t =30–50 min), CckA localizes uniformly in the cell. CckA relocates to the old pole in the stalked stage (t = 50–90 min) and becomes bipolar in the early pre-divisional stage (t = 90–120 min). DivL exhibits uniform localization except in the early pre-divisional stage, when it relocates to the new pole.

The other two species, DivK and CtrA and their phosphorylated forms, diffuse rapidly within the cell. Fluorescence microscopy indicates that DivK shuttles from one end of the cell to the other within 5 s [29]. With the formula $d^2 = 2Dt$, where $d = 1.3\ \mu$m is the size of the cell and $t = 5$ s, we can calculate the diffusion constant of DivK as $\frac{d^2}{2t} \approx 10\mu m^2 \cdot \text{min}^{-1}$. We use the same diffusion constant for CtrA.

References

[1] Abel S, Bucher T, Nicollier M, Hug I, Kaever V, Abel Z W P and Jenal U 2013 Bi-modal distribution of the second messenger c-di-GMP controls cell fate and asymmetry during the caulobacter cell cycle *PLoS Genet.* **9** e1003744

[2] Aldridge P, Paul R, Goymer P, Rainey P and Jenal U 2003 Role of the GGDEF regulator PleD in polar development of *Caulobacter crescentus Mol. Microbiol.* **47** 1695–708

[3] Angelastro P S, Sliusarenko O and Jacobs-Wagner C 2010 Polar localization of the CckA histidine kinase and cell cycle periodicity of the essential master regulator CtrA in *Caulobacter crescentus J. Bacteriol.* **192** 539–52

[4] Bernstein J A, Khodursky A B, Lin P H, Lin-Chao S and Cohen S N 2002 Global analysis of mRNA decay and abundance in *Escherichia coli* at single-gene resolution using two-color fluorescent dna microarrays *Proc. Natl Acad. Sci.* **99** 9697–702

[5] Biondi E G, Reisinger S J, Skerker J M, Arif M, Perchuk B S, Ryan K R and Laub M T 2006 Regulation of the bacterial cell cycle by an integrated genetic circuit *Nature* **444** 899–904

[6] Bowman G R, Lyuksyutova A I and Shapiro L 2011 Bacterial polarity *Curr. Opin. Cell Biol.* **23** 71–7

[7] Chen Y E, Tsokos C G, Biondi E G, Perchuk B S and Laub M T 2009 Dynamics of two Phosphorelays controlling cell cycle progression in *Caulobacter crescentus J. Bacteriol.* **191** 7417–29

[8] Collier J, Murray S R and Shapiro L 2006 DnaA couples DNA replication and the expression of two cell cycle master regulators *EMBO J.* **25** 346–56

[9] Collier J and Shapiro L 2007 Spatial complexity and control of a bacterial cell cycle *Curr. Opin. Biotechnol.* **18** 333–40

[10] Curtis P D and Brun Y V 2010 Getting in the loop: Regulation of development in *Caulobacter crescentus Microbiol. Mol. Biol. Rev.* **74** 13–41

[11] dos Santos V T, Bisson-Filho A W and Gueiros-Filho F J 2012 DivIVA-mediated polar localization of ComN, a posttranscriptional regulator of *Bacillus subtilis J. Bacteriol.* **194** 3661–9

[12] Duerig A, Abel S, Folcher M, Nicollier M, Schwede T, Amiot N, Giese B and Jenal U 2009 Second messenger-mediated spatiotemporal control of protein degradation regulates bacterial cell cycle progression *Genes Dev.* **23** 93–104

[13] Gardiner C, McNeil K, Walls D and Matheson I 1976 Correlations in stochastic theories of chemical reactions *J. Stat. Phys.* **14** 307–31

[14] Gillespie D T 1976 A general method for numerically simulating the stochastic time evolution of coupled chemical reactions *J. Comput. Phys.* **22** 403–34

[15] Gillespie D T 1977 Exact stochastic simulation of coupled chemical reactions *J. Phys. Chem.* **81** 2340–61

[16] Holtzendorff J, Hung D, Brende P, Reisenauer A, Viollier P H, McAdams H H and Shapiro L 2004 Oscillating global regulators control the genetic circuit driving a bacterial cell cycle *Science* **304** 983–7

[17] Hung D Y and Shapiro L 2002 A signal transduction protein cues proteolytic events critical to *Caulobacter* cell cycle progression *Proc. Natl Acad. Sci.* **99** 13160–5

[18] Iniesta A A, McGrath P T, Reisenauer A, McAdams H H and Shapiro L 2006 A phospho-signaling pathway controls the localization and activity of a protease complex critical for bacterial cell cycle progression *Proc. Natl Acad. Sci.* **103** 10935–40

[19] Isaacson S A 2009 The reaction–diffusion master equation as an asymptotic approximation of diffusion to a small target *SIAM J. Appl. Math.* **70** 77–111

[20] Isaacson S A 2013 A convergent reaction–diffusion master equation *J. Chem. Phys.* **139** 054101

[21] Jacobs C, Hung D and Shapiro L 2001 Dynamic localization of a cytoplasmic signal transduction response regulator controls morphogenesis during the *Caulobacter* cell cycle *Proc. Natl Acad Sci. USA* **98** 4095–100

[22] Jenal U and Fuchs T 1998 An essential protease involved in bacterial cell-cycle control *EMBO J.* **17** 5658–69

[23] Jenal U and Galperin M Y 2009 Single domain response regulators: molecular switches with emerging roles in cell organization and dynamics *Curr. Opin. Microbiol.* **12** 152–60

[24] Judd E M, Ryan K R, Moerner W E, Shapiro L and McAdams H H 2003 Fluorescence bleaching reveals asymmetric compartment formation prior to cell division in *Caulobacter Proc. Natl Acad Sci.* **100** 8235–40

[25] Lam H, Matroule J-Y and Jacobs-Wagner C 2003 The asymmetric spatial distribution of bacterial signal transduction proteins coordinates cell cycle events *Dev. Cell* **5** 149–59

[26] Laub M T, Shapiro L and McAdams H H 2007 Systems biology of *Caulobacter Annu. Rev. Genet.* **41** 429–41

[27] Chen M, Li F, Wang S and Cao Y Stochastic simulation of Hill function in reaction-diffusion systems *Third International workshop on computational network biology: Modeling, Analysis, and Control* (*CNB-MAC 2016*) (submitted)

[28] Lin Y, Crosson S and Scherer N F 2010 Single-gene tuning of *Caulobacter* cell cycle period and noise, swarming motility, and surface adhesion *Mol. Syst. Biol.* **6** 445

[29] Matroule J-Y, Lam H, Burnette D T and Jacobs-Wagner C 2004 Cytokinesis monitoring during development: rapid pole-to-pole shuttling of a signaling protein by localized kinase and phosphatase in *Caulobacter Cell* **118** 579–90

[30] McGrath P T, Iniesta A A, Ryan K R, Shapiro L and McAdams H H 2006 A dynamically localized protease complex and a polar specificity factor control a cell cycle master regulator *Cell* **124** 535–47

[31] Milo R, Jorgensen P, Moran U, Weber G and Springer M 2010 Bionumbers—the database of key numbers in molecular and cell biology *Nucleic Acids Res.* **38** (Suppl .1) D750–3

[32] Munro E and Bowerman B 2009 Cellular symmetry breaking during *Caenorhabditis elegans* development *Cold Spring Harbor Perspect. Biol.* **1** a003400

[33] Paul R, Jaeger T, Abel S, Wiederkehr I, Folcher M, Biondi E G, Laub M T and Jenal U 2008 Allosteric regulation of histidine kinases by their cognate response regulator determines cell fate *Cell* **133** 452–61

[34] Paul R, Abel S, Wassmann P, Beck A, Heerklotz H and Jenal U 2007 Activation of the diguanylate cyclase PleD by phosphorylation-mediated dimerization *J. Biol Chem.* **282** 29170–7

[35] Pedraza J M and Paulsson J 2008 Effects of molecular memory and bursting on fluctuations in gene expression *Science* **319** 339–43

[36] Petricka J J, Van Norman J M and Benfey P N 2009 Symmetry breaking in plants: Molecular mechanisms regulating asymmetric cell divisions in *Arabidopsis Cold Spring Harbor Perspect. Biol.* **1** a000497

[37] Prehoda K E 2009 Polarization of Drosophila neuroblasts during asymmetric division *Cold Spring Harbor Perspect. Biol.* **1** a001388

[38] Ptacin J L, Lee S F, Garner E C, Toro E, Eckart M, Comolli L R, Moerner W and Shapiro L 2010 A spindle-like apparatus guides bacterial chromosome segregation *Nat. Cell Biol.* **12** 791–8

[39] Quon K C, Yang B, Domian I J, Shapiro L and Marczynski G T 1998 Negative control of bacterial DNA replication by a cell cycle regulatory protein that binds at the chromosomeorigin *Proc. Natl Acad. Sci.* **95** 120–5

[40] Schofield W B, Lim H C and Jacobs-Wagner C 2010 Cell cycle coordination and regulation of bacterial chromosome segregation dynamics by polarly localized proteins *EMBO J.* **29** 3068–81

[41] Siegal-Gaskins D and Crosson S 2008 Tightly regulated and heritable division control in single bacterial cells *Biophys. J.* **95** 2063–72

[42] Stein G, van Wijnen A, Stein J, Lian J, Montecino M, Choi J, Zaidi K and Javed A 2000 Intranuclear trafficking of transcription factors: implications for biological control *J. Cell Sci.* **113** 2527–33 http://www.ncbi.nlm.nih.gov/pubmed/10862710

[43] Subramanian K, Paul M R and Tyson J J 2013 Potential role of a bistable histidine kinase switch in the asymmetric division cycle of *Caulobacter crescentus PLoS Comput. Biol.* **9** e1003221

[44] Subramanian K, Paul M R and Tyson J J 2015 Dynamical localization of DivL and PleC in the asymmetric division cycle of *Caulobacter crescentus*: a theoretical investigation of alternative models *PLoS Comput. Biol.* **11** e1004348

[45] Taniguchi Y, Choi P J, Li G-W, Chen H, Babu M, Hearn J, Emili A and Xie X S 2010 Quantifying *E. coli* proteome and transcriptome with single-molecule sensitivity in single cells *Science* **329** 533–8
[46] Thanbichler M 2009 Spatial regulation in *Caulobacter crescentus Curr. Opin. Microbiol.* **12** 715–21
[47] Tsokos C, Perchuk B and Laub M 2011 A dynamic complex of signaling proteins uses polar localization to regulate cell-fate asymmetry in *Caulobacter crescentus Developmental Cell* **20** 329–41
[48] Wheeler R T and Shapiro L 1999 Differential localization of two histidine kinases controlling bacterial cell differentiation *Mol. Cell* **4** 683–94
[49] Wu L J and Errington J 2003 RacA and the Soj-Spo0J system combine to effect polar chromosome segregation in sporulating *Bacillus subtilis Mol. Microbiol.* **49** 1463–75
[50] Zenklusen D, Larson D R and Singer R H 2008 Single-RNA counting reveals alternative modes of gene expression in yeast *Nat. Struct. Mol. Biol.* **15** 1263–71